

# Investigation on ultra-compact 2D-PC based optical circulator for photonic integrated circuits

R. ARUNKUMAR, S. ROBINSON\*

*Department of Electronics and Communication Engineering, Mount Zion College of Engineering and Technology, Pudukkottai-622 507, Tamil Nadu, India*

In this attempt, Two Dimensional Photonic Crystals (2DPC) based three-port and four-port circulator are proposed and designed. The performance parameters of circulators namely, insertion loss, isolation and transmission efficiency are estimated. The circulator is designed using a square lattice of silicon rods in the air. In this structure, a defect is introduced which is made of ferrite material to obtain the non-reciprocal transmission of the optical signal. The Photonic Band Gap (PBG) range of the device is accomplished through Plane Wave Expansion (PWE) method and by applying the Finite Difference Time Domain (FDTD) method the transmission spectra of the proposed circulator are obtained. The size of the circulator is about  $12\mu\text{m}\times 12\mu\text{m}$ . The proposed device will be used for future optical networks and telecommunication applications.

(Received March 14, 2020; accepted April 8, 2021)

*Keywords:* Photonic crystal, Photonic band gap, Circulator, PWE, FDTD, Ferrite materials

## 1. Introduction

The non-reciprocal components used in fiber optical communication systems are enormous. An optical circulator is employed to separate the optical signals while traveling in an optical fiber [1]. In the earliest technology, researchers have designed optical devices in the range of centimeter (cm) and millimeter (mm) through MEMS technology. Recently the optical devices are designed using Photonic Crystal (PC) in the range of nanometer (nm). Generally, PC is a periodic dielectric material that has Photonic Band Gap (PBG). In PBG, a certain wavelength range of light is not traveled inside the structure which is allowed by incorporating defects. The PC based optical devices provide better performance and suitable for many applications. [2-3]. There are several PC based optical devices are reported namely, sensor [4], demultiplexer [5] etc.

In the literature, the circulator is designed using square and triangular lattice by incorporating either line defects or point defects using T type, Y type, Windmill type and cross-type [6-26]. Edward Yung et al. were designed a Y-junction circulator by using a magnetized ferrite sphere for millimeter-wave applications [8]. Keyu Tao et al. were proposed high efficiency circulator using T-Shape with side coupled cavity and coupled magneto-optical rods which were formed by varying the radius and refractive index of the defect. The insertion losses and isolation have arrived at 0.24 dB and 20 dB, respectively [9]. Victor Dmitriev, Gianni Portela et al, were proposed the circulator based on T-Shape using magneto-optical resonator is reported to operate in sub THZ and THZ frequency range and it offered the isolation of about 15 dB [10].

Biaogang Xu et al. designed the device by introducing a defect in square lattice magneto-photonic pillar array, a T-shaped waveguide circulator was designed using cylindrical ferrite rods which provide the isolation of 25.92 dB and insertion loss of 0.064 dB [11]. Guohua Wen et al. devised a highly compact circulator with an insertion loss of 0.02 dB and isolation of 46 dB in a square lattice. It was formed and implemented by a magneto-optical rod in different wavebands [12]. Guoliang Zheng et al. designed the 6 port circulator using magneto-optical rods. The insertion loss and isolation were about 0.017 dB and 29 dB, respectively [13].

Alexander V. Baryshev et al. were demonstrated a four-port circulator which is based on a 2D magneto photonic crystal slab-hexagonal array made of a Bismuth-substituted Yttrium iron garnet rod. It was provided isolation of 16 dB [14]. An optical circulator is formed by magneto-optical cavity is reported, where 30dB isolation is estimated at 1550nm [15]. Zheng Wang et al. designed four-port circulator by time-reversal symmetry breaking magneto-optical photonic crystal. The isolation is 26 dB was reported [16]. Victor Dmitriev, Gianni Portela et al. were designed three-port circulator using magneto-optical resonator with hexagonal and square lattice [17]. Further, many authors were designed three-port and four-port circulators using square and triangular lattice and its functional parameters namely, insertion loss and isolation were estimated [18-23].

Typically, square lattice based PCs have several advantages such as low out-of-plane losses, propagation loss, easy fabrication, compatible with classical PICs, and effective single mode operation due to defects based structure [2]. Two dimensional (2D) PCs are receiving keen attention by the scientific community as they have attractive features including relatively simple fabrication,

better confinement of light, efficient PBG calculation, effective control of spontaneous emission and easy integration with other devices [3]. Owing to the above advantages, 2D square lattice is conceived for circulator design.

In the literature so far, various unique attempts are made to devise a photonic crystal based circulator. However, still improvements in functional parameters such as isolation, insertion loss and transmission efficiency are required. In this attempt, a three-port and four-port circulator is proposed using square lattice by incorporating ferrite material as a point defect. The defect based structure is considered as it provides high isolation and high transmission efficiency. The functional parameters namely transmission efficiency, insertion loss and isolation are investigated.

The other part of this manuscript is organized as follows; the band diagram, scattering matrix and material properties of the ferrite materials are presented in Section 2. The structural design of the three-port circulator and its obtained results through simulation are illustrated in Section 3. Section 4 gives the structural design of the four-port circulator and its results. Finally, the conclusion is discussed in Section 5.

## 2. Theoretical analysis

### 2.1. Scattering matrix

A circulator is a matched, lossless but non-reciprocal three-port and four-port device, whose scattering matrix is ideally given by,

$$[S]= \begin{pmatrix} s_{11} & s_{12} & s_{13} \\ s_{21} & s_{22} & s_{23} \\ s_{31} & s_{32} & s_{33} \end{pmatrix} \quad (1)$$

By applying the unitary condition in equation 1,

$$S_{12}S_{12}^* + S_{13}S_{13}^* = 1 \quad (2)$$

$$S_{21}S_{21}^* + S_{23}S_{23}^* = 1 \quad (3)$$

$$S_{31}S_{31}^* + S_{32}S_{32}^* = 1 \quad (4)$$

In a three-port circulator, the signal is coming out to Port 2 while applying the input at Port 1 and the output is reached if the signal is given at Port 2 and vice versa. The scattering matrix for an ideal three-port circulator is

$$[S]= \begin{pmatrix} 0 & 0 & s_{13} \\ s_{21} & 0 & 0 \\ 0 & s_{32} & 0 \end{pmatrix} \quad (5)$$

By applying,  $S_{12}=S_{23}=S_{31}=0$  and  $S_{21}=S_{32}=S_{13}=1$

$$[S]= \begin{pmatrix} 0 & 0 & 1 \\ 1 & 0 & 0 \\ 0 & 1 & 0 \end{pmatrix} \quad (6)$$

The ferrite rod incorporated at the center of the device and the following equation is employed to get magnetic permeability and permittivity.

$$[\mu]=\mu_0 \begin{pmatrix} \mu & -ik & 0 \\ ik & \mu & 0 \\ 0 & 0 & \mu \end{pmatrix}; \quad \varepsilon=12.5\varepsilon_0 \quad (7)$$

where  $\mu$  and  $k$  are given by,

$$\mu = 1 + \frac{\omega_m(\omega_i + j\omega\alpha)}{(\omega_i + j\omega\alpha)^2 - \omega^2} \quad (8)$$

$$k = \frac{\omega_m\omega}{(\omega_i + j\omega\alpha)^2 - \omega^2} \quad (9)$$

The terms  $\omega_m$  and  $\omega_i$  are defined as,

$$\omega_m = \gamma M_0 \quad (10)$$

$$\omega_i = \gamma H_0 \quad (11)$$

where,  $\mu_0$  - free-space magnetic permeability,  $H_0$  - applied DC magnetic field,  $M_0$  - saturation magnetization,  $\alpha$  - damping factor,  $\gamma$ - gyromagnetic ratio,  $\omega$ -radian frequency.

### 2.2 Gap map and photonic band gap

The unique structure for PC based circulator is designed on a square lattice with silicon rods in the background of air. The lattice constant is about 540nm denoted as 'a'. The silicon rods have radii of 0.1 $\mu$ m and the value of the refractive index is 3.46 ( $\Delta=2.46$ ), where it is denoted as 'r' and  $\Delta$ , respectively. The structural parameter values, namely, refractive index, rod radius and lattice constant are used to design the proposed circulator which is obtained through a gap map. The Plane Wave Expansion (PWE) method is employed to determine the PBG of the proposed device.

The propagation mode of the periodic structure and PBG are shown in Fig. 1. The band diagram has two PBG for TE mode and the details of this TE PBG are listed in Table 1. The TE PBG over the wavelength range of 1239nm to 1826nm is accounted for here.

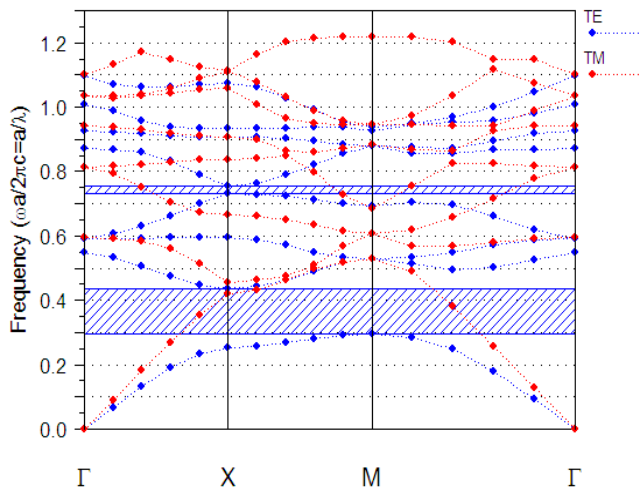


Fig. 1 Band diagram of the proposed circulator (color online)

Table 1. Type of PBG, normalized frequency and its wavelength range

PBG	Normalized Frequency	Wavelength
TE	0.2958a/λ to 0.4359a/λ	1239nm to 1826nm
	0.7317a/λ to 0.7551a/λ	715nm to 738nm

### 2.3. Types of circulator

Generally, in PCs, there are four types of three port circulators are reported based on their shapes namely (a) T-shaped circulator, (b) Windmill-shaped circulator, (c) Y-shaped circulator and (d) W shaped circulator. The schematic structure of the above mentioned types of three-port circulators is shown in Figs. 2(a)-(d). Naturally, three-port circulator is composed of three waveguides and a resonator. As the waveguides are formed in T-shape, it is called a T-shaped circulator. It is made through a square lattice as shown in Fig. 2(a). Here, the bend of light has occurred  $90^\circ$  from one port to another. Windmill-shaped structure shown in Fig. 2(b), in this, there are three waveguides which exhibit  $120^\circ$  in respect to the center cavity. The schematic of a Y-shaped structure has three branches with  $120^\circ$  rotation, shown in Fig. 2(c) and a W-shaped circulator is obtained by altering the location of port 3 of the Y-shaped circulator. The port 3 of Y-shaped circulator is located between port 1 and port 2 at the angle distance of  $60^\circ$ . The W-shaped circulator is offering a very small size owing to it's the orientation of its port, shown in Fig. 2(d). Among all, T-shaped circulators provide significant in performance enhancement. Hence, it is considered in this attempt.

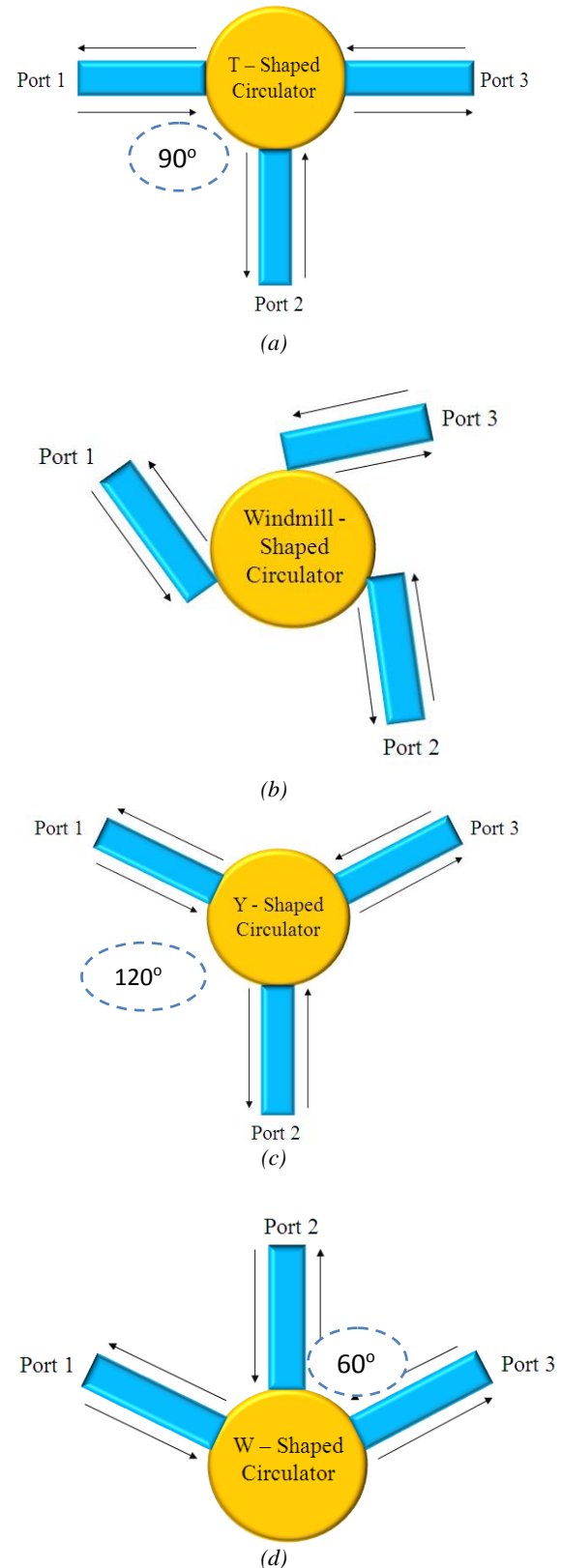


Fig. 2. Schematic structure of (a) T-shaped circulator, (b) Windmill shaped circulator, (c) Y-shaped circulator and (d) W-shaped circulator (color online)

### 3. Design of three port circulator

Figs. 3 (a) and (b) show the structural design of the three-port circulator and a sectional view of the micro cavity. It consists of three waveguides and a cavity, where the waveguide is designed through line defects (by removal of rods in a row) and the cavity is formed through point defects (by changing the radius of the rod). It has three ports namely input port, output port and isolated port, when the input port has changed the output and isolated port are also changed. The point defect in the ring resonator is incorporated by varying the refractive index and rod radius, which is located at the center. The outer rod is made of ferrite material to couple two ports, which leads to  $90^\circ$  rotation of light transmission from one port to another port at a particular wavelength. The refractive index of ferrite material is 3.67 and the center rod is made of silicon material whose refractive index is 3.46. The radius of the outer rod and the center rod is about 100nm and 65nm, respectively. In addition, an attempt is made by having a different ferrite outer rod radius and the ferrite center rod radius of the proposed circulators. It is investigated that the transmission efficiency, insertion loss and isolation are varied significantly while changing the radius of ferrite rod other than 100nm and 65nm. The radius of ferrite rods are selected by considering the maximum transmission efficiency, minimum insertion loss and better isolation. The Perfect Matched Layer (PML) is incorporated in order to minimize the back reflections. The size of the PML layer is selected as 500nm.

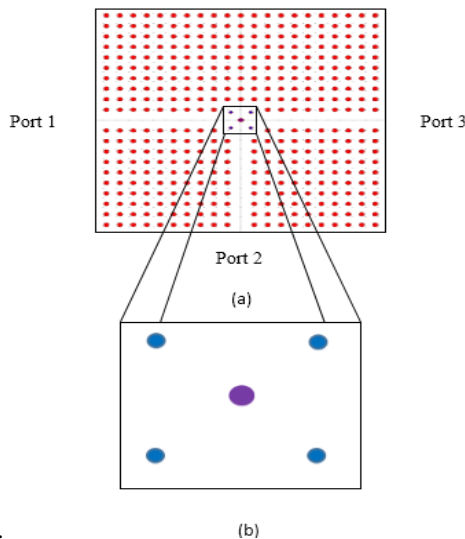


Fig. 3(a) Structural design of three-port circulator and (b) sectional view of micro cavity (color online)

The Gaussian input signal is applied to the input port. The output response is attained at the output port using Fast Fourier Transform (FFT) which is determined by the 2D FDTD method. The power monitor is employed both in the input and output port to estimate the normalized output response. The electric field distribution of the proposed three-port circulator from port 1-2, port 2-3 and port 3-1 are shown in Figs. 4(a), (b) and (c), respectively.

From Fig. 4, it is observed that when the input signal is applied at port 1, it is coupled to port 2 without reaching port 3. Likewise when the signal is applied at port 2, it is reached port 3, however, the signal is not coupling port 1 and vice versa. The transmission efficiency, isolation and insertion loss are one of the important parameters of the circulator. The isolation and insertion loss is calculated using the following formula;

$$\text{Isolation} = 10 \log_{10} (P_{in}/P_{iso}) \text{ dB} \quad (12)$$

$$\text{Insertion loss} = 10 \log_{10} (P_{in}/P_{out}) \text{ dB} \quad (13)$$

where  $P_{in}$ ,  $P_{out}$  and  $P_{iso}$  have denoted the power from the transmitting port, output port and isolated port, respectively.

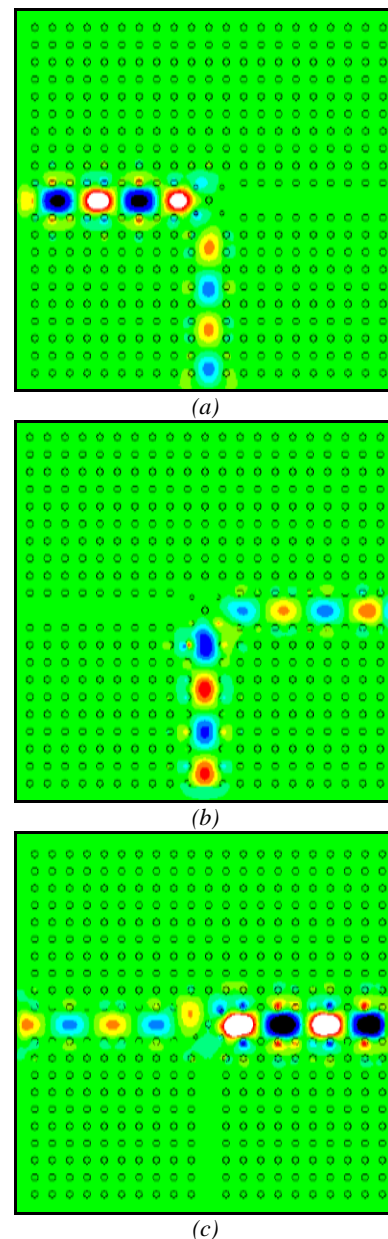


Fig. 4. Field distribution of three-port circulator at 1550 nm from (a) Port 1-2 (b) Port 2-3 and (c) Port 3-1 (color online)

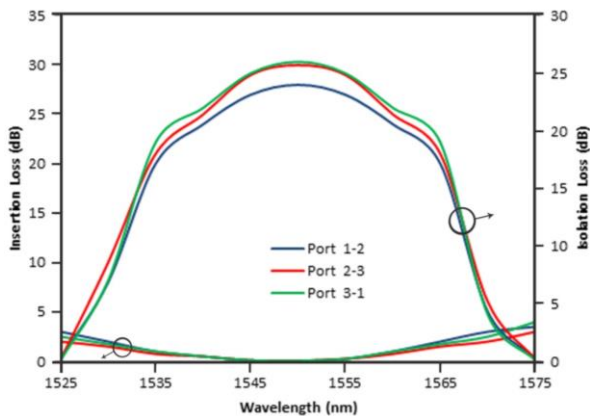


Fig. 5. Insertion loss and isolation of three-port circulator (color online)

Fig. 5 depicts the isolation and insertion loss of the proposed circulator. The functioning wavelength range of the circulator is from 1525nm to 1570nm. The transmission efficiency is varying about 85% to 95% from one port to other ports. Similarly the minimum insertion loss is around 0.05dB. The isolation is around 27dB to 30dB which is highly sufficient to realize a real device. The proposed three-port circulator design is extended to design four-port circulator, which is discussed in the next Section.

#### 4. Design of four port circulator

Fig. 6, shows the structural design of four-port circulator. It has four waveguides and a cavity. The material properties and radius of the rods are similar to three-port circulators. The field pattern of the four-port circulator from ports 1-2, 2-3, 3-4 and 4-1 is shown in Fig. 7(a), (b), (c) and (d).

The isolation and insertion loss of the proposed four port circulator is shown in Fig. 8. The working wavelength range of the circulator is varying from 1525nm to 1570nm. The transmission efficiency is varying about 85% to 95%. Similarly the minimum insertion loss is around 0.05dB. The isolation is around 25dB to 28dB.

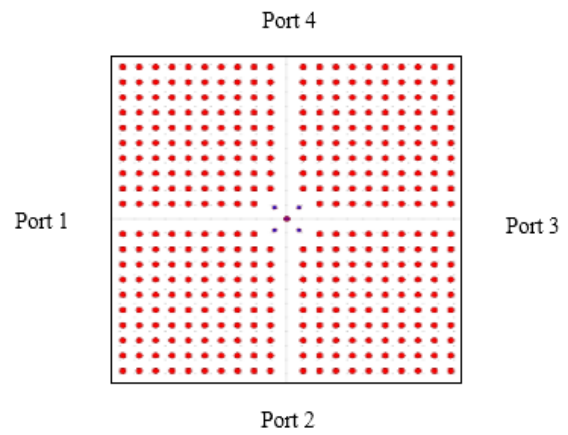


Fig. 6. Structural design of four-port circulator (color online)

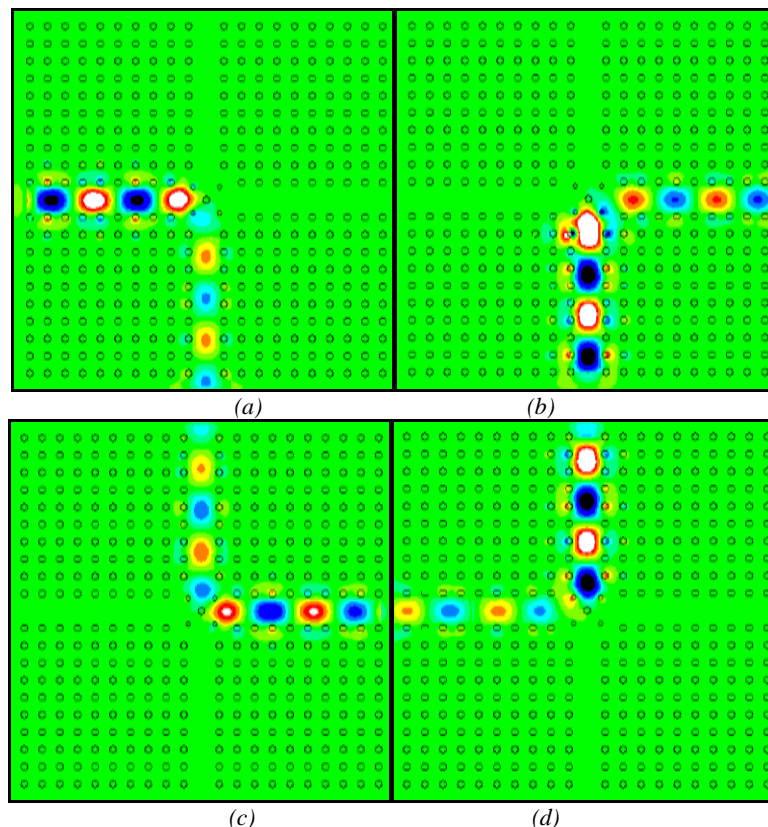


Fig. 7 Field distribution of four-port circulator at 1550nm (a) Port 1-2 (b) Port 2-3 (c) Port 3-4 and (d) Port 4-1 (color online)

The functional parameters of the three-port and four-port circulator are namely, transmission efficiency, insertion loss and isolation are listed in Table 2. It is witnessed that the average transmission efficiency is about 95%. The isolation and insertion loss of the circulator is 28dB and 0.05dB, respectively. As the proposed circulator is fulfilling the requirements to transfer the signal with good functional characteristics, it would be accounted for future optical networks for photonic integrated circuits.

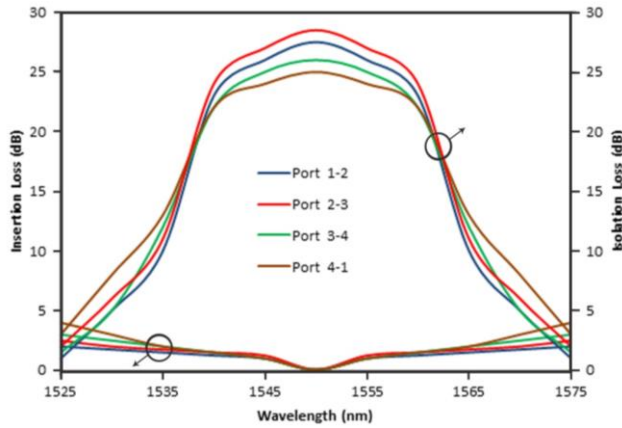


Fig. 8. Insertion loss and isolation of four-port circulator (color online)

Table 2. Transmission efficiency, insertion loss and isolation of three-port circulator and four-port circulator

Parameters	Three-Port Circulator			Four-Port Circulators			
	Port 1-2	Port 2-3	Port 3-1	Port 1-2	Port 2-3	Port 3-4	Port 4-1
Transmission Efficiency	95%	95%	95%	95%	92%	95%	95%
Insertion Loss (dB)	0.05	0.05	0.05	0.06	0.08	0.06	0.06
Isolation (dB)	27	29	30	27	28	26	25

Table 3. Functional parameters comparison of proposed circulators with existing circulators

Authors/Year	Lattice Structure	Structure Type	No of Ports	Insertion Loss	Isolation
Ref. 15	Hexagonal	Windmill type	Three port	-	30 dB
Ref. 26	Hexagonal	Windmill type	Three port	9 dB	16dB
Ref. 09	Square	T type	Three port	0.23 dB	20.45 dB
Ref. 13	Hexagonal	Star type	Six port	0.017 dB	29 dB
Ref. 11	Square	T type	Three port	0.064 dB	25.92 dB
Ref. 12	Square	Cross type	Four port	0.02 dB	46 dB
Ref. 10	Square	T type	Three port	0.45 dB	15 dB
Ref. 20	Hexagonal	Y type	Three port	0.45 dB	15 dB
Ref. 18	Square	T type	Four port	0.3 dB	15 dB
Ref. 21	Square	Cross type	Four port	--	--
Ref. 17	Hexagonal	Y type	Three port	0.021dB	--
Ref. 22	Square	T type	Four port	0.04 dB	28 dB
Ref. 23	Hexagonal	Y type	Three port	0.05 dB	25 dB
Ref. 24	Square	Cross type	Four port	--	--
In this work	Square	T type and cross type	Three port and four port	0.05-0.08 dB	24-30 dB

The functional characteristics of the proposed four-port circulators are compared with reported circulators which are itemized in Table 3. From Table 3, it is investigated that there is a better amount of insertion loss and isolations reported, however, the transmission efficiency and device size are larger. Alternatively, if the transmission efficiency is larger, it is offered a higher value of insertion loss and isolation. It is clearly seen that the proposed circulator accomplishes better than the reported one and the size is very small hence it will be suitable for optical networks.

## 5. Conclusions

In this paper, a design and analysis of two dimensional photonic crystal based three-port and four-port circulator with point defect have been attempted and examined through the 2D-FDTD method. The transmission efficiency, insertion loss and isolation of the proposed three-port and four-port circulator are 95%, 0.05 dB, 29 dB and 95%, 0.08 dB, 28 dB, respectively. The functioning wavelength range of the proposed circulator is spanning from 1525nm and 1570nm. The overall size of the circulator is around  $12\mu\text{m}\times 12\mu\text{m}$ . Hence, the devised circulators can be useful for photonic integrated circuits.

## References

- [1] Miller, S. E. Weiss, Bell system technical journal **10**(1002), 1538 (1995).
- [2] A. A. M. Kok, J. J. G. M. Van der Tol, Roel Baets, M. K. Smit, Journal of Lightwave Technology **27**(17), 3904 (2009).
- [3] John D. Joannopoulos, Joshua N. Winn, Robert D. Mead, Photonic crystals: Molding the flow of light, Princeton Press, Princeton, NJ, 1995.
- [4] J. D. Joannopoulos, Pierre R. Villeneuve, Shanhui Fan, Nature **386**, 143 (1997).
- [5] S. Rajaseker, S. Robinson, Plasmonics **14**(1), 3 (2018).
- [6] K. Venkatachalam, D. Sriram Kumar, S. Robinson, Optoelectronics Review **26**(2), 108 (2018).
- [7] S. Robinson, R. Nakkeeran, Optik **124**(5), 393 (2013).
- [8] Edward K. N. Yung, D. G. Zhang, Roger S. K. Wong, Microwave theory and techniques **44**(3), 454 (1996).
- [9] Keyu Tao, Mi Lin, Qiong Wang, Zhengbiao Ouyang, Journals of Physics Letter A **10**(1016), 646 (2012).
- [10] Victor Dmitriev, Gianni Portela, Leno Martins, Victor Dmitriev, Journal of Optics **15**(8), 1 (2015).
- [11] Biaogang Xu, Dengguo Zhang, Shixiang Xu, Tan Huang, Yong Wang, IEEE Photonics Journal **5**(2), 518060 (2014).
- [12] Guohua Wen, Jingjing Wang, Qiong Wang, Xin Jin, Zhengbiao Ouyang, Journal of PLOS **10**(1371), 1 (2014).
- [13] Guoliang Zheng, Mi Lin, Qiong Wang, Yaoxian Zheng, Zhengbiao Ouyang, Journals of the Magnetism Society of Japan **30**(6), 1 (2015).
- [14] Alexander V. Baryshev, Kazuo Ya Yoi, Kazuma Tobinaga, Journal of Applied Physics **109**(750), 0021 (2011).
- [15] Shanhui Fan, Zheng Wang, Journal of Optics Letters **30**(15), 151989 (2010).
- [16] Zheng Wang, Shanhui Fan, Photonics and Nanostructures **10**(1016), 132 (2016).
- [17] C. Umamaheswari, D. Shanmugasundar, A. Sivanantha Raja, Journal of Optics Communication **382**, 186 (2017).
- [18] Victor Dmitriev, Gianni Portela, Leno Martins, Photonic Network Communications **33**(3), 303 (2017).
- [19] Yong Wang, Dengguo Zhang, Shixiang Xu, Zhengbiao Ouyang, Jingzhen Li, Optics Communication **369**, 1 (2017).
- [20] Victor Dmitriev, Gianni Portela, Leno Martins, Photonic Network Communications **31**(1), 56 (2016).
- [21] M. Djavid, M. H. T. Dastjerdi, M. R. Philip, D. D. Choudhary, A. Khreishah, H. P. T. Nguyen, Optik **144**, 586 (2017).
- [22] Xiang Xi, Mi Lin, Wenbiao Qiu, Zhengbiao Ouyang, Qiong Wang, Qiang Liu, Results in Physics **7**, 4303 (2017).
- [23] Xiang Xi, Mi Lin, Wenbiao Qiu, Zhengbiao Ouyang, Qiong Wang, Qiang Liu, Scientific Reports **8**(1), 7827 (2018).
- [24] K. Prabu, Dhanashree Nasre, Plasmonics **14**(2), 1261 (2019).
- [25] Yong Wang, Dengguo Zhang, Shixiang Xu, Biaogang Xu, Zheng Dong, Tan Huang, Optoelectron. Adv. Mat. **12**(5-6), 283 (2018).
- [26] Yayoi, Kazuo, Tobinaga, Kazuma Kaneko, Yusuke Baryshev, Alexander Inoue, Mitsuteru, Journal of Applied Physics **109**(7), 07B750-1 (2011).

\*Corresponding author: mail2robinson@gmail.com